Understanding the Scattering Transform using Univariate Signals

Youngmi Hur
Department of Mathematics,
Yonsei University,
Seoul, Korea
yhur@yonsei.ac.kr

Hyojae Lim
Department of Mathematics,
Yonsei University,
Seoul, Korea
hyo5064@yonsei.ac.kr

***Abstract*—In this paper, we review the scattering transform in the univariate setting. After reviewing its properties including translation invariance, stability under small diffeomorphism, and ability to carry high-frequency information, we investigate how these properties can be used in understanding the effect of the scattering transform when various types of signal deformation are considered. We find that, together with the Fourier transform modulus, the scattering transform can be used in classifying some of these deformations.**

I. Introduction

Image or sound is typical signal information. Often, this information does not change with translation, or rotation, and it is stable under small diffeomorphism.

For example, a picture of cat is the same cat picture whether we translate it or rotate it. Also, we can recognize it as a cat picture even though we smoothly crease the picture.

The scattering transform in [1] is introduced motivated by this observation. It is shown to be translation invariant, and stable under small diffeomorphism, and to carry high-frequency information. It is also shown that the scattering transform can capture the interference when several signals are synthesized [2]. Therefore, we may say that the scattering transform plays a role of an indicator capturing important information of the data.

There exist other transforms that play a similar role but they are limited in the sense that they satisfy only part of the above properties. For example, the Fourier transform modulus is translation invariant but it is not stable under small diffeomorphism.

The scattering transform is used in applications, for example, in image classification [3], [4] and for learning data on graph [5], often outperforming the state-of-art methods currently used in those applications.

Although the scattering transform can be applied to the data in any dimension, and it can be used in combination with a finite group or even with a compact Lie group such as the rotation group, in this paper, we concentrate on the univariate setting and do not combine with the rotation group since in the univariate case the rotation group becomes trivial.

We review the background of the scattering transform and look into the principles how they can lead to the scattering transform satisfying all the properties mentioned above. Then, by concrete examples through MATLAB, we gain the understanding of the scattering transform as an indicator when applied for the univariate data. In particular, we go beyond the specific form of deformation studied in [1], which is referred to as the diffeomorphism in the paper and also as the elastic translation in [2]. We consider not only this elastic translation type but also other ways such as the additive and multiplicative type to deform signals, both smoothly and non-smoothly, and investigate how they behave under the scattering transform. We discuss how the scattering transform, with the help of the Fourier transform modulus, can be used in classifying some of these deformations.

II. Scattering Transform

In this section, we review the scattering transform. We start with the wavelet system which plays an essential role in defining the scattering transform in Section II-A. In Section II-B and Section II-C, we present some of the main ingredients that are helpful in understanding the scattering transform. Finally, in Section II-D, we present the definition of the scattering transform and discuss its properties.

A. Wavelets for Scattering Transform

In the scattering transform, a wavelet system generated by dilating a mother wavelet $\psi \in L^2(\mathbb{R})$ is used. In the sense that only the dilation operator is used, instead of both the dilation and the translation operators being used, it is not the most common form of wavelet systems that are used nowadays (see, for example, [6] or [7]). This wavelet system has been used in the literature, especially in connection with the Littlewood-Paley theory [8].

Let $\psi \in L^1(\mathbb{R}) \cap L^2(\mathbb{R})$ be a mother wavelet of the form $\psi(x) = e^{i\eta x}\theta(x)$ with $\hat{\psi}(0) = 0$, where $\eta \in \mathbb{R}$ and $\hat{\theta}(\omega)$ is a real-valued function concentrated on a ball centered at 0 with radius of order of π. Here and below, we use the notation $\hat{f}$ to denote the Fourier transform of f, i.e. $\hat{f}(w) := \int f(x)e^{-ixw}dx$. Then $\hat{\psi}(\omega) = \hat{\theta}(\omega - \eta)$, which means that the frequency of ψ is concentrated on the ball centered at η with the same radius of $\hat{\theta}$.

The wavelet system is obtained from a mother wavelet by dilating at a scale of 2^j for $j \in \mathbb{Z}$. More precisely, we let $\Lambda_\infty := 2^{\mathbb{Z}}$, and define ψ_λ, $\lambda = 2^j \in \Lambda_\infty$, as the dilated

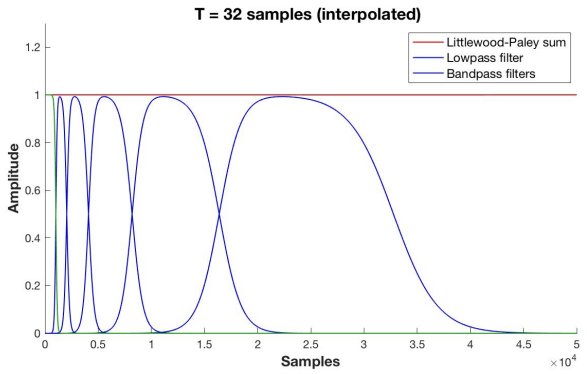

Fig. 1. Littlewood-Paley condition

wavelet with a scale 2^{-j}, i. e. $\psi_\lambda(x) := 2^j\psi(2^j x)$. Then $\hat{\psi}_\lambda(\omega) = \hat{\psi}(2^{-j}\omega) = \hat{\psi}(\lambda^{-1}\omega) = \hat{\theta}(\lambda^{-1}\omega - \eta)$, which means that the frequency of ψ_λ is concentrated in the ball centered at $\lambda\eta$ with a radius proportional to 2^j. Thus, ψ_λ can be considered as the band frequency filter associated with λ.

For a wavelet system $\{\psi_\lambda\}_{\lambda\in\Lambda_\infty}$, the wavelet transform of $f \in L^2(\mathbb{R})$ is defined as

$$W[\lambda]f := f * \psi_\lambda = \int f(u)\psi_\lambda(\cdot - u)du.$$

The wavelet transform is used in defining the prototype operator W_J of the one-step propagator U_J (c.f. (5)), which is used in defining the windowed scattering transform (see Section II-B). The prototype operator W_J at a scale 2^J keeps wavelets with frequency dilation $2^j > 2^{-J}$ only. The lower frequencies which cannot be covered by these wavelets can be expressed by averaging over the spatial domain proportional to 2^J, as in $A_J f = f * \phi_{2^J}$ with $\phi_{2^J}(x) := 2^{-J}\phi(2^{-J}x)$, where the averaging function ϕ satisfies $|\hat{\phi}(\omega)|^2 = \sum_{j=-\infty}^{0} |\hat{\psi}(2^{-j}\omega)|^2$. Thus,

$$W_J f := \{A_J f, (W[\lambda]f)_{\lambda\in\Lambda_J}\}$$

where

$$\Lambda_J := \{\lambda = 2^j : 2^j > 2^{-J}\} \subset \Lambda_\infty. \tag{1}$$

We further assume that $|\hat{\phi}(0)| = 1$, and for a.e. $w \in \mathbb{R}$,

$$|\hat{\phi}(2^J\omega)|^2 + \sum_{j>-J} |\hat{\psi}(2^{-j}\omega)|^2 = 1. \quad \forall J \in \mathbb{Z},$$

which is referred to as the Littlewood-Paley condition in [1].

Figure 1 shows how the Littlewood-Paley condition is satisfied for the orthogonal Battle-Lemarié cubic spline wavelet, which is the mother wavelet we use for the scattering transform in all of our experiments in this paper. The Littlewood-Paley condition guarantees the operator W_J, and hence U_J as well, to be unitary operator on $L^2(\mathbb{R})$.

If, in addition, the functions ϕ and ψ satisfy twice differentiability together with certain decay conditions (which we choose not to explicitly write – see [1] for details), the associated scattering transform can be shown to be Lipschitz-continuous under diffeomorphism, which is used to gain the stability under small diffeomorphism in [1]. We will discuss more about this in Section II-D.

Furthermore, in order to guarantee that the windowed scattering transform preserves the norm of the original function, ψ has to be admissible (again, we do not explicitly write the condition here, and refer the readers to [1] for details).

Lastly, $|\hat{\psi}(\omega)| \neq 0$ a.e should be satisfied in order for the measures of cylinders of finite paths (c.f. (6) and (7)) not to vanish, which is essential in defining the scattering transform.

One of the examples satisfying all of the above conditions is the orthogonal Battle-Lemarié cubic spline wavelet [9], [10], and we use this wavelet for all of our experiments in Section III.

B. Scattering Propagator and Windowed Scattering Transform

Let us consider the translation-invariant property. Since the integral of the operator which commutes with translations is translation-invariant, and since the wavelet transform is commuting with translation, the integral of the wavelet transform will be translation-invariant. However, since $\hat{\psi}(0) = 0$, the integral of the wavelet transform vanishes everywhere because

$$\int (f * \psi)(x)\, dx = 0.$$

To resolve this matter, the modulus of the wavelet transform can be taken as the function which commutes with translations rather than the wavelet transform itself. However, this still has a problem because all the frequencies except zero will be lost as can be seen from

$$\int |(f * \psi)(x)|\, dx = \widehat{|f * \psi|}(0).$$

By obtaining the modulus of the wavelet transform several times along several frequencies, such lost high-frequency information can be recovered [3].

A (unit-length) scattering propagator $U[\lambda]$ is first defined as the modulus of the wavelet transform along a 'unit-length' frequency (c.f. (2)), and it commutes with translations. By using a path, which enumerates several frequencies in a fixed order, the (generalized) scattering propagator $U[\lambda_1, \lambda_2, \cdots, \lambda_m]$ (c.f. (3)) can be defined for finite-length freqencies, and it also commutes with translations. The windowed scattering transform will be defined by integrating a scattering propagator defined along a frequency path over a localized space and by weakening that localization, the operator will be translation-invariant.

A path, which can be comparted by the length, is defined as follows. Each element $\lambda = 2^j \in \Lambda_\infty$ will be called as a unit-length path. For each $m \in \mathbb{N}$, m-length path p is an ordered sequence of length m, which is an element of $\Lambda_\infty^m := \{p = (\lambda_1, \lambda_2, \cdots, \lambda_m) : \lambda_i \in \Lambda_\infty, \forall i\}$. We would consider a path of 0-length, which we call an empty path $\emptyset$, and denote also as $\Lambda_\infty^0 := \emptyset$. A collection of finite paths $\mathcal{P}_\infty$ is the union of Λ_∞^m for all $m \in \mathbb{N} \cup \{0\}$. That is, $\mathcal{P}_\infty = \bigcup_{m\in\mathbb{N}\cup\{0\}} \Lambda_\infty^m$. An

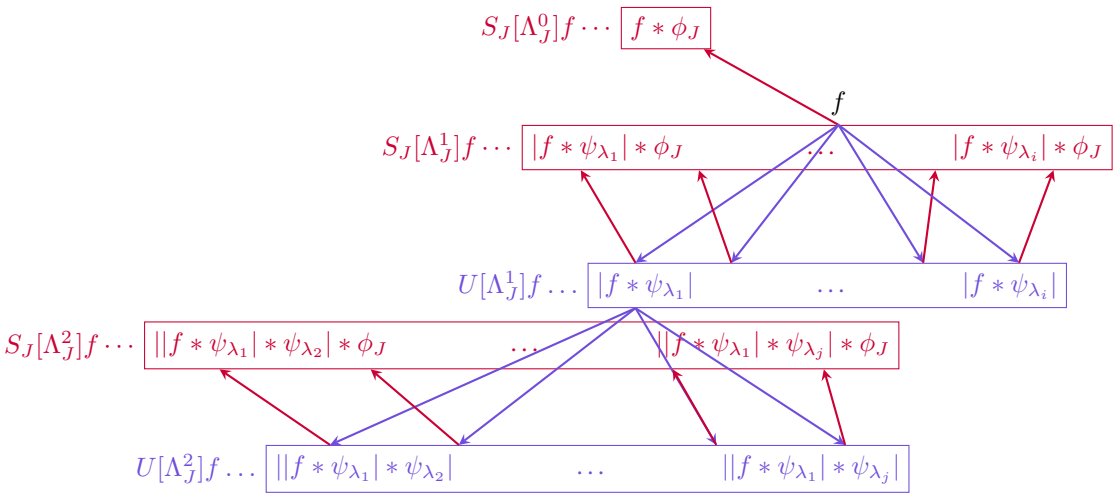

Fig. 2. Scattering propagator along several finite paths

infinite-length path is an infinite ordered sequence which is an element of an infinite product Λ_∞^∞ of Λ_∞.

A scattering propagator $U[\lambda]$ over a unit-length path λ is defined as the modulus of the wavelet transform: For $f \in L^2(\mathbb{R})$ and $\lambda \in \Lambda_\infty$,

$$U[\lambda]f := |f * \psi_\lambda|. \tag{2}$$

For a positive length path $p = (\lambda_1, \lambda_2, \cdots, \lambda_m) \in \mathcal{P}_\infty \backslash \Lambda_\infty^0$, a (generalized) scattering propagator $U[p]$ is defined as

$$U[p] := U[\lambda_m] \cdots U[\lambda_2]U[\lambda_1].$$

That is, for $f \in L^2(\mathbb{R})$,

$$U[p]f = ||f * \psi_{\lambda_1}| * \psi_{\lambda_2}| * \cdots | * \psi_{\lambda_m}|. \tag{3}$$

Also, for an empty path $\emptyset = \Lambda_\infty^0 \subset \mathcal{P}_\infty$, we would define the scattering propagator $U[\emptyset]$ as $U[\emptyset]f := f$, for $f \in L^2(\mathbb{R})$.

Recall that for $J \in \mathbb{Z}$, Λ_J defined in (1) is a unit-length path whose frequency is restricted. We let $\Lambda_J^0 := \emptyset$ as well, and define Λ_J^m, for $m \in \mathbb{N}$, and $\mathcal{P}_J$ in a similar fashion, using Λ_J in place of Λ_∞, so that each of these collections contains only a path with frequency higher than 2^{-J}.

For $p \in \mathcal{P}_J$ and $f \in L^2(\mathbb{R})$, the windowed scattering transform $S_J[p]f$ is defined as

$$S_J[p]f := (U[p]f) * \phi_{2^J} = \int U[p]f(u)\phi_{2^J}(\cdot - u)du. \tag{4}$$

For fixed $J \in \mathbb{Z}$, the one-step propagator U_J (similar to the previous W_J) is defined as follows: For $f \in L^2(\mathbb{R})$,

$$U_J f := \{A_J f, (U[\lambda]f)_{\lambda \in \Lambda_J}\}. \tag{5}$$

Using the windowed scattering operator, it can be written as

$$U_J f = \{S_J[\emptyset]f, (U[\lambda]f)_{\lambda \in \Lambda_J}\}.$$

After applying the one-step propagator to a function f, applying the operator again to $(U[\lambda]f)_{\lambda \in \Lambda_J}$ gives, for each $\lambda \in \Lambda_J$,

$$U_J(U[\lambda]f) = \{A_J(U[\lambda]f), (U[\lambda'](U[\lambda]f))_{\lambda' \in \Lambda_J}\},$$

which can also be written as

$$U_J(U[\lambda]f) = \{S_J[\lambda]f, (U[\lambda, \lambda']f)_{\lambda' \in \Lambda_J}\}.$$

The one-step propagator can be iteratively applied to $U[p]f$ and this process is illustrated in Figure 2.

The windowed scattering transform S_J can be considered as a localization of the scattering transform over the spatial domain proportional to 2^J. As J goes to ∞, the spatial localization of the windowed scattering transform may be weakened. Observing this property, the scattering transform $\overline{S}$ is defined. Its definition and the fact that for $f \in L^2(\mathbb{R})$ with certain conditions, $\overline{S}f$ lies in a Hilbert space generated from a path space $\overline{\mathcal{P}}_\infty$ will be discussed in Section II-D. The definition of $\overline{\mathcal{P}}_\infty$, and a measure for it will be discussed in the next subsection.

C. Path Space and Measure for Scattering Transform

In this subsection, $\overline{\mathcal{P}}_\infty$, the limit of the frequency path sets $\mathcal{P}_J$, will be defined and the measure on the limit will be introduced.

For any two paths $p = (\lambda_1, \cdots, \lambda_m), p' = (\lambda_1', \cdots, \lambda_n')$ of finite length, the addition can be defined by concatenating:

$$p + p' := (\lambda_1, \cdots, \lambda_m, \lambda_1', \cdots, \lambda_n')$$

Hence, for a unit-length path λ, $p + \lambda := (\lambda_1, \cdots, \lambda_m, \lambda)$.

Since we have $\mathcal{P}_J \subset \mathcal{P}_{J+1}$ for all $J \in \mathbb{Z}$, for any $p \in \mathcal{P}_J$, p can be extended in $\mathcal{P}_{J+1}$ to $p + 2^{-J}$. This path $p + 2^{-J}$ can be further extended in $\mathcal{P}_{J+2}$ to $p + 2^{-J} + 2^{-(J+1)}$.

By repeating this process as follows

$$\begin{array}{ccccccc} \mathcal{P}_J & \subset & \mathcal{P}_{J+1} & \subset & \mathcal{P}_{J+2} & \subset & \cdots \\ \cup & & \cup & & \cup & & \\ p & \longmapsto & p + 2^{-J} & \longmapsto & p + 2^{-J} + 2^{-(J+1)} & \longmapsto & \cdots, \end{array}$$

infinitely many times, p can be extended to a path of infinite-length. Therefore, as J increases, this process will prolong the

paths and $\overline{\mathcal{P}}_\infty$, the limit of the path set $\mathcal{P}_J$, should contain the infinite-length paths, and it is easily seen that $\overline{\mathcal{P}}_\infty = \mathcal{P}_\infty \cup \Lambda_\infty^\infty$.

Since Λ_∞ is a discrete subset of $\mathbb{R}$, the discrete topology is used on Λ_∞. Then, since the infinite-length path set Λ_∞^∞ is defined by ordered products of Λ_∞, open sets of Λ_∞^∞ have cylinderical shapes: For each $\lambda \in \Lambda_\infty$ and $n \geq 0$, let

$$\mathcal{C}_n(\lambda) := \{p = (\lambda_1, \lambda_2, \cdots) \in \Lambda_\infty^\infty : p_{n+1} = \lambda\}$$

be an open element of Λ_∞^∞ which is referred to as a cylinder.

Since each cylinder set $\mathcal{C}_n(\lambda_1', \lambda_2', \cdots, \lambda_m') := \{p = (\lambda_1, \lambda_2, \cdots) \in \Lambda_\infty^\infty : \lambda_{n+1} = \lambda_1', \lambda_{n+2} = \lambda_2', \cdots, \lambda_{n+m} = \lambda_m'\}$ is a finite intersection of open cylinders as in

$$\mathcal{C}_n(\lambda_1, \lambda_2, \cdots, \lambda_m) = \bigcap_{i=1}^{m} \mathcal{C}_{n+i}(\lambda_i),$$

cylinder sets are both open and closed, and thus, the topology is a σ-algebra and a measure can be defined.

Also, for the finite path set $\mathcal{P}_\infty$, the appropriate cylinder set can be associated with $p = (\lambda_1, \lambda_2, \cdots, \lambda_n) \in \mathcal{P}_\infty$ as follows:

$$C(p) := \mathcal{C}_0(p) = \{q \in \Lambda_\infty^\infty : q_1 = \lambda_1, q_2 = \lambda_2, \cdots, q_n = \lambda_n\},$$

where $q = (q_1, q_2, \cdots)$ and q_i's are all unit-length paths. Note that for each $p \in \mathcal{P}_\infty$, $C(p) \subset \overline{\mathcal{P}}_\infty$.

Since open cylinders $\mathcal{C}_n(\lambda)$ can be expressed as a union of cylinder sets, $\mathcal{C}_n(\lambda) = \bigcup_{(\lambda_1, \lambda_2, \cdots, \lambda_n) \in \Lambda_\infty^n} C(\lambda_1, \lambda_2, \cdots, \lambda_n, \lambda)$, two sets, $C(\cdot)$ and $\mathcal{C}_n(\cdot)$, will generate the same σ-algebra.

Thus, for all $p = (\lambda_1, \lambda_2, \cdots, \lambda_m) \in \mathcal{P}_\infty$, a σ-finite Borel measure μ can be defined as

$$\mu(C(p)) := \|U[p]\delta\|^2, \tag{6}$$

where $U[p]\delta = ||\psi_{\lambda_1}| * \psi_{\lambda_2}| * \cdots | * \psi_{\lambda_m}|$.

Cylinder sets of frequency resolution can be defined as follows: For each $J \in \mathbb{Z}$,

$$C_J(p) := \bigcup_{\lambda \in \Lambda_\infty, |\lambda| \leq 2^{-J}} C(p + \lambda) \subset C(p).$$

Also, note that for each $p \in \mathcal{P}_\infty$, $C_J(p) \subset \overline{\mathcal{P}}_\infty$ for all $J \in \mathbb{Z}$.

Since $C_J(p)$ is defined by using the cylinder sets $C(\cdot)$ without frequency resolution, the measure on $C_J(p)$ can be derived (c.f. Proposition 3.2 in [1]) by using the measure in (6): For all $p \in \mathcal{P}_\infty$,

$$\mu(C_J(p)) = \|S_J[p]\delta\|^2. \tag{7}$$

Since $C(p)$, $C_J(p) \subset \overline{\mathcal{P}}_\infty$ for each $p \in \mathcal{P}_\infty$ and for all $J \in \mathbb{Z}$, all paths in $\mathcal{P}_\infty$ can be embedded to $\overline{\mathcal{P}}_\infty = \mathcal{P}_\infty \cup \Lambda_\infty^\infty$ through two types of cylinders $C(p)$ and $\{C_J(p)\}_{J \in \mathbb{Z}}$.

Then, the distance between q and q' for $q, q' \in \overline{\mathcal{P}}_\infty$ can be defined as follows by using (7): For any distinct $q, q' \in \overline{\mathcal{P}}_\infty$,

$$d(q, q') := \inf_{q, q' \in C_J(p)} \mu(C_J(p)),$$

and $d(q, q) := 0$. It can be shown that $\overline{\mathcal{P}}_\infty$ is complete with this metric.

D. Definition and Properties of Scattering Transform

Using the windowed scattering transform $S_J[p]f$, a new function $S_J f$ on $\overline{\mathcal{P}}_\infty \times \mathbb{R}$ is defined as

$$S_J f(q, x) := \sum_{p \in \mathcal{P}_J} \frac{S_J[p]f(x)}{\|S_J[p]\delta\|} \mathbb{1}_{C_J(p)}(q),$$

where $\mathbb{1}_{C_J(p)}$ is the characteristic function on $C_J(p)$ in $\overline{\mathcal{P}}_\infty$.

The windowed scattering transform $S_J[p]f$ averages $U[p]f$ over the spatially localized space depending on J. As J goes to ∞, the windowed scattering transform loses the spatial localization. (i.e. loses the spatial variable 'x' dependence.) By using the marginal $L^2(\mathbb{R})$ norm of $S_J f(q, x)$ along x for fixed q, define

$$\overline{S}_J f(q) := \int |S_J f(q, x)|^2 \, dx = \sum_{p \in \mathcal{P}_J} \frac{\|S_J[p]f\|}{\|S_J[p]\delta\|} \mathbb{1}_{C_J(p)}(q),$$

which depends only on the path variable 'q'. After all, it can be shown (c.f. Theorem 3.5 in [1]) that for all $f \in L^2(\mathbb{R})$ and $q \in \overline{\mathcal{P}}_\infty$, $\overline{S}_J f(q)$ converges strongly as J goes to ∞ with Condition (3.15) at [1] satified in a dense set of $L^2(\mathbb{R})$, and this limit is defined as the scattering transform $\overline{S}f(q)$. It can further be shown that $\overline{S}f \in L^2(\overline{\mathcal{P}}_\infty, d\mu)$ with norm denoted by $\|\cdot\|_{\overline{\mathcal{P}}_\infty}$.

We now study the properties of the scattering transform $\overline{S}$. Suppose that $f, h \in L^2(\mathbb{R})$ satisfy Condition (3.15) in [1]. Then by Theorem 3.5 in [1] again, we have

$$\left\|\overline{S}f - \overline{S}h\right\|_{\overline{\mathcal{P}}_\infty} = \lim_{J \to \infty} \|S_J[\mathcal{P}_J]f - S_J[\mathcal{P}_J]h\|,$$

where $S_J[\mathcal{P}_J]f := \{S_J[p]f\}_{p \in \mathcal{P}_J}$. Thus, the scattering transform $\overline{S}$ can inherit the properties of $S_J[\mathcal{P}_J]$. Properties of $S_J[\mathcal{P}_J]$ include the following:

1) Translation invariance: Let $L_c f(x) := f(x - c)$ be the translation of $f \in L^2(\mathbb{R})$ about $c \in \mathbb{R}$. Then (c.f. Theorem 2.10 in [1]), for all $f \in L^2(\mathbb{R})$ and $c \in \mathbb{R}$,

$$\lim_{J \to \infty} \|S_J[\mathcal{P}_J]f - S_J[\mathcal{P}_J]L_c f\| = 0.$$

2) Stability under small diffeomorphism: Lipschitz continuity can be used to guarantee the stability under the small diffeomorphism. The windowed scattering transform has Lipschitz continuity under a small C^2-diffeomorphism τ of $\mathbb{R}$ sufficiently close to a translation (c.f. Theorem 2.12 in [1]): For all $f \in L^2(\mathbb{R})$ with $\|U[\mathcal{P}_J]f\|_1 := \sum_{m=0}^{\infty} \|U[\Lambda_J^m]f\| < \infty$ and for all $\tau \in C^2(\mathbb{R})$ with $\|\nabla\tau\|_\infty \leq \frac{1}{2}$, there exists a constant c such that

$$\|S_J[\mathcal{P}_J]L_\tau f - S_J[\mathcal{P}_J]f\| \leq c \|U[\mathcal{P}_J]f\|_1 K(\tau),$$

where $L_\tau f(x) := f(x - \tau(x))$ and

$$K(\tau) := 2^{-J}\|\tau\|_\infty + \|\nabla\tau\|_\infty \max\left(\log \frac{\|\Delta\tau\|_\infty}{\|\nabla\tau\|_\infty}, 1\right) + \|H\tau\|_\infty,$$

with $\|\Delta\tau\|_\infty := \sup_{x,u \in \mathbb{R}} |\tau(x) - \tau(u)|$ and $H\tau$ being the Hessian tensor of τ.

From the above results, we see that the scattering transform is translation invariant and stable under small diffeomorphism.

III. Scattering Transform under Deformation

In this section, we study how the scattering transform behaves under different kind of deformations of the data.

The idea is that when a signal is deformed, often, we do not have the information about the type of deformation. We try to find out which type of deformation is underwent by observing the behaviors of the scattering transform and the Fourier transform modulus of each deformed signal.

We consider three different types of signal deformation. The first one is the elastic translation considered in [1], [2]. The elastic translation considered in these papers is the smooth deformation. In this paper, we will consider the non-smooth elastic translation as well. The second type we consider is the additive deformation, and the third type is the multiplicative deformation.

Whereas the deformation by the elastic translation is made through the 'domain' of the signal $f(x)$ as in the form of $f(x-g(x))$ where $g(x)$ is an appropriate deformation function, the other two types are obtained by adding or multiplying the deformation function $g(x)$ on the 'range' of the signal $f(x)$ as in the form of $f(x)+g(x)$ or $f(x)g(x)$.

One can consider the deformation function $g(x)$ of the form $g_\alpha(x) = (1-\alpha)s(x)+\alpha e(x)$, where α is a number in between 0 and 1, and $s(x)$ is a smooth function, and $e(x)$ is a non-smooth function. In this paper, to simplify our discussion, we concentrate the two cases only; when $\alpha = 0$, i.e., $g_0 = s$, which would express a smooth deformation, and when $\alpha = 1$, i.e. $g_1 = e$, which would express a non-smooth deformation.

Throughout this section,the scattering transform obtained by the orthogonal Battle-Lemarie cubic spline wavelet will be used. In order to simplify the discussion, we fix the signal f and the smooth function s as $f(x) = 3\cos 14x + \sin 5x$ and $s(x) = 1/(1+\exp(-x))$. We note that the smooth function s here satisfies the properties that the diffeomorphism τ needs to satisfy for the Lipschitz continuity of the scattering transform (c.f. Section II-D). The non-smooth function e is defined as the absolute value of a Gaussian noise function [11], taken from the Gaussian distribution with mean 0 and variance $\frac{1}{25}$. We further normalize e so that $\|e\|_\infty \approx 0.7\,\|s\|_\infty$ for the smooth function s fixed as above, since, with this normalization, we find the two functions are visually comparable.

A. Deformation Type 1: Elastic Translation

The signal deformation by the first type, the elastic translation with a deformation function g_α, can be expressed as

$$D_{1,\alpha}f(x) := f(x - g_\alpha(x)), \qquad \text{for } \alpha = 0 \text{ or } 1.$$

The graph of the original signal f and deformed signals $D_{1,0}f$, $D_{1,1}f$ are shown in the top row of Figure 3. The figures in the middle row show the scattering transform $\overline{S}f$, $\overline{S}(D_{1,0}f)$, and $\overline{S}(D_{1,1}f)$, and the bottom row shows the Fourier modulus $|\widehat{f}|$, $|\widehat{D_{1,0}f}|$ and $|\widehat{D_{1,1}f}|$. We see that $\overline{S}f$ and $\overline{S}(D_{1,0}f)$ are very similar as the theory of [1] guarantees, but $\overline{S}(D_{1,1}f)$ is different from $\overline{S}f$ since the function e used for the elastic translation in this case is not smooth.

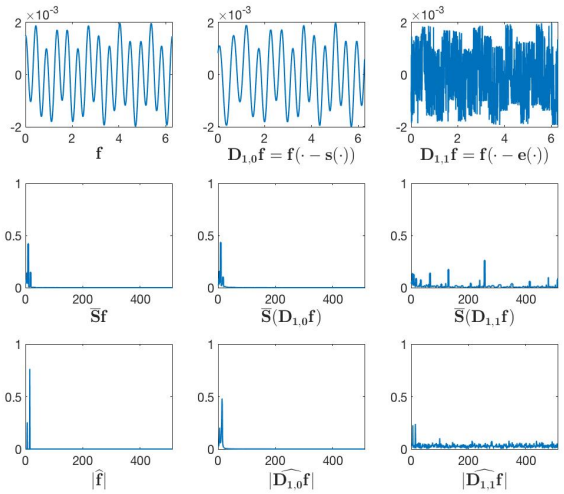

Fig. 3. Scattering transform and Fourier modulus under the elastic translation studied in Section III-A

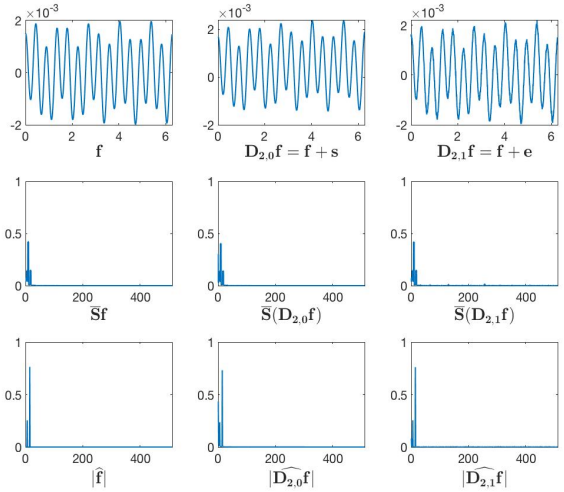

Fig. 4. Scattering transform and Fourier modulus under the additive deformation studied in Section III-B

By using the measure of the path space discussed earlier in Section II-C, it can be shown that the x-axis of the scattering transform is designed to contain the frequency information (c.f. Section 3.3 in [1]). This can be observed by comparing the graphs in the second row with the ones in the third row of Figure 3. We see that where the scattering transform and the Fourier modulus are supported are the same although the value of the two transforms differ.

B. Deformation Type 2: Additive Deformation

The signal deformation of the additive type has the form

$$D_{2,\alpha}f(x) := f(x) + g_\alpha(x), \qquad \text{for } \alpha = 0 \text{ or } 1.$$

The top row of Figure 4 shows the graph of the original function f, and additively deformed signals $D_{2,0}f$ and $D_{2,1}f$.

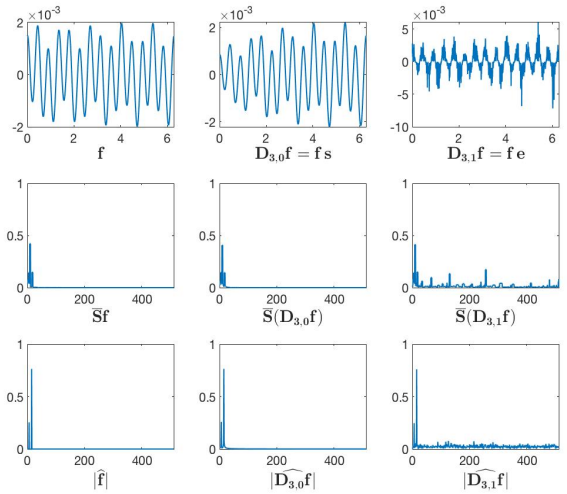

Fig. 5. Scattering transform and Fourier modulus under the multiplicative deformation studied in Section III-C

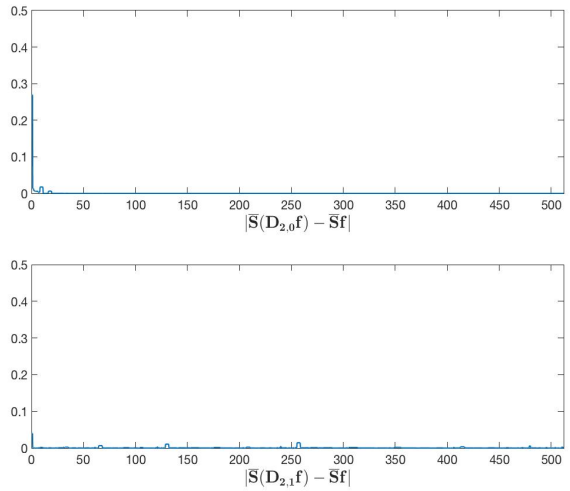

Fig. 6. Scattering differences $|\overline{S}(D_{2,0}f) - \overline{S}f|$, $|\overline{S}(D_{2,1}f) - \overline{S}f|$ with $D_{2,0}f$, $D_{2,1}f$ deformed additively (c. f. Sections III-B and III-D)

The middle row shows the graphs of the scattering transform $\overline{S}f$, $\overline{S}(D_{2,0}f)$ and $\overline{S}(D_{2,1}f)$. The bottom row shows the graph of the Fourier modulus $|\widehat{f}|$, $|\widehat{D_{2,0}f}|$ and $|\widehat{D_{2,1}f}|$. In this case, the scattering transform of the deformed signals look similar to that of the original signal. However, a closer look at the differences $|\overline{S}(D_{2,0}f) - \overline{S}f|$ and $|\overline{S}(D_{2,1}f) - \overline{S}f|$ in Figure 6 reveals that $|\overline{S}(D_{2,0}f) - \overline{S}f|$ shows the low frequency content more strongly, which indicates the smooth deformation, whereas the frequency content of $|\overline{S}(D_{2,1}f) - \overline{S}f|$ is spread out, which indicates the non-smooth deformation.

C. Deformation Type 3: Multiplicative Deformation

The multiplicative type deformation can be expressed as

$$D_{3,\alpha}f(x) := f(x)g_\alpha(x), \qquad \text{for } \alpha = 0 \text{ or } 1.$$

Figure 5 shows the result about the multiplicative deformation. In top figures, the original signal f and deformed signals $D_{3,0}f$, $D_{3,1}f$ can be seen. The middle graphs show the scattering transforms $\overline{S}f$, $\overline{S}(D_{3,0}f)$ and $\overline{S}(D_{3,1}f)$. The bottom graphs show the Fourier modulus $|\widehat{f}|$, $|\widehat{D_{3,0}f}|$ and $|\widehat{D_{3,1}f}|$. From these graphs, we see that the scattering transform of the smoothly deformed $D_{3,0}f$ is almost the same as that of f. However, the scattering transform of the non-smoothly deformed $D_{3,1}f$ changes a lot from that of f. A closer look at the differences $|\overline{S}(D_{3,0}f) - \overline{S}f|$ and $|\overline{S}(D_{3,1}f) - \overline{S}f|$ shown in Figure 7 confirms these observations.

D. Classifying Signal Deformation

Now we discuss ways to classify the deformations by observing the scattering transform and the Fourier modulus of each deformed signal.

First of all, whether the deformation is performed by the smooth function or the non-smooth function can be determined easily by comparing the scattering transform results $\overline{S}(D_{i,0}f)$ and $\overline{S}(D_{i,1}f)$ for type $i = 1, 2, 3$ deformation, shown in

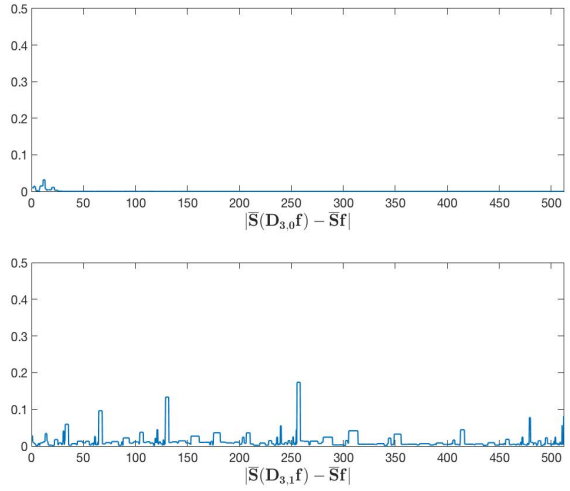

Fig. 7. Scattering differences $|\overline{S}(D_{3,0}f) - \overline{S}f|$, $|\overline{S}(D_{3,1}f) - \overline{S}f|$ with $D_{3,0}f$, $D_{3,1}f$ deformed multiplicatively (c. f. Sections III-C and III-D)

Figure 3, Figure 4, and Figure 5, respectively. Since the smooth deformation modifies the original signal smoothly, the change would occur at the front side of x-axis, which corresponds to the low frequency content (if it occurs at all). On the other hand, the way the non-smooth deformation modifies the signal is less regular, resulting the change to spread out throughout the whole x-axis.

Figure 6 depicts the scattering differences $|\overline{S}(D_{2,0}f) - \overline{S}f|$, $|\overline{S}(D_{2,1}f) - \overline{S}f|$ for additive deformation, and Figure 7 depicts the scattering differences $|\overline{S}(D_{3,0}f) - \overline{S}f|$, $|\overline{S}(D_{3,1}f) - \overline{S}f|$ for multiplicative deformation. We are able to classify the smooth deformation of additive type and multiplicative type by comparing $|\overline{S}(D_{2,0}f) - \overline{S}f|$ in Figure 6 with $|\overline{S}(D_{3,0}f) - \overline{S}f|$ in Figure 7. A large value exists at the front part of the graph

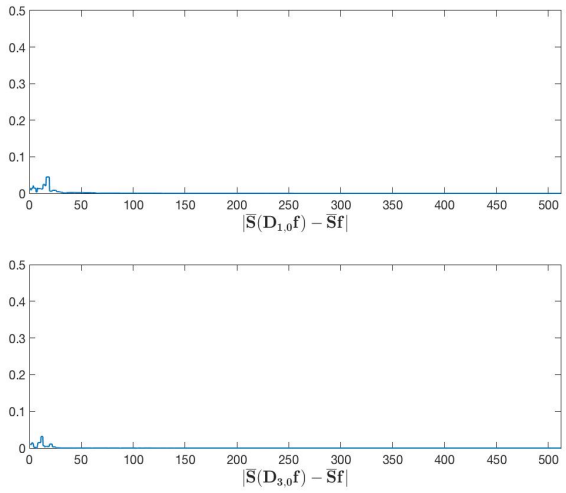

Fig. 8. Scattering differences $|\overline{S}(D_{1,0}f) - \overline{S}f|$, $|\overline{S}(D_{3,0}f) - \overline{S}f|$ with the smooth deformation, by the elastic translation and the multiplicative types

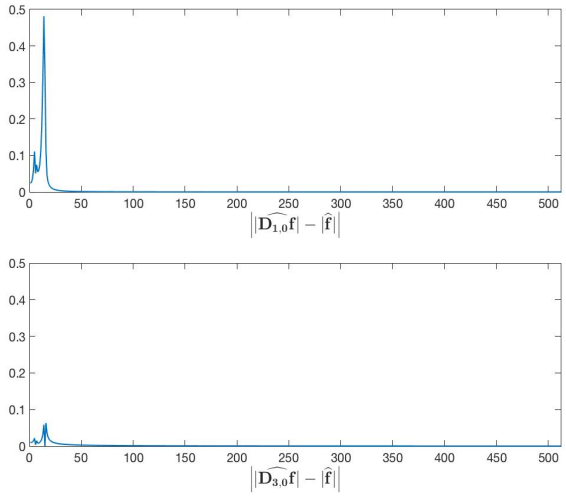

Fig. 9. Fourier modulus differences $\left||\widehat{D_{1,0}f}| - |\widehat{f}|\right|$, $\left||\widehat{D_{3,0}f}| - |\widehat{f}|\right|$ with the smooth deformation, by the elastic translation and the multiplicative types

in $|\overline{S}(D_{2,0}f) - \overline{S}f|$, but not in $|\overline{S}(D_{3,0}f) - \overline{S}f|$.

Now let us think about how one can distinguish the smooth deformation between the elastic translation type and the multiplicative type. Comparing the scattering differences $|\overline{S}(D_{1,0}f) - \overline{S}f|$ (for the elastic translation) and $|\overline{S}(D_{3,0}f) - \overline{S}f|$ (for the multiplicative deformation) in Figure 8 does not seem to give meaningful information in distinguishing the two. In this case, we find that comparing the difference of Fourier modulus is more informative. Fourier modulus differences $\left||\widehat{D_{1,0}f}| - |\widehat{f}|\right|$ (for the elastic translation) and $\left||\widehat{D_{3,0}f}| - |\widehat{f}|\right|$ (for the multiplicative deformation) in Figure 9 are clearly different. Therefore, in this case, by comparing the difference of Fourier modulus, it is possible to classify the multiplicative type and the elastic translation type.

IV. Conclusion

In this paper, we reviewed the scattering transform in the univariate setting by presenting main ingredients toward understanding its theory. We then studied the effect of the scattering transform under various types of signal deformation, and suggested some new ways to classify several deformations through the scattering transform and the Fourier modulus.

Acknowledgment

This research was supported in part by the National Research Foundation of Korea (NRF) [Grant Number 20151009350].

References

[1] Stéphane Mallat. *Group invariant scattering*, Communications on Pure and Applied Mathematics, 65 (10) (2012): 1331-1398.

[2] Stéphane Mallat. *Recursive interferometric representation*, European Signal Processing Conference (EUSIPCO), Denmark, August (2010).

[3] Joan Bruna, Stéphane Mallat. *Classification with scattering operators*, IEEE Computer Vision and Pattern Recognition (CVPR), June (2011): 1561-1566.

[4] Joan Bruna, Stéphane Mallat. *Invariant scattering convolution networks*, IEEE Transactions on Pattern Analysis and Machine Intelligence, 35 (8) (2013): 1872-1886.

[5] Xu Chen, Xiuyuan Cheng, and Stéphane Mallat. *Unsupervised deep haar scattering on graphs*, Advances in Neural Information Processing Systems 27 (NIPS), (2014):1709-1717.

[6] Ingrid Daubechies. *Ten Lectures on Wavelets*, Society for Industrial and Applied Mathematics, (1992).

[7] Gilbert Strang, Truong Nguyen. *Wavelets and Filter banks*, Society for Industrial and Applied Mathematics, (1996).

[8] Michael Frazier, Björn Jawerth, and Guido Weiss. *Littlewood-Paley theory and the study of function spaces*, American Mathematical Society, (79) (1991).

[9] Guy Battle. *A block spin construction of ondelettes. I. Lemarié functions*, Communications in Mathematical Physics, 110 (4) (1987): 601-615.

[10] Pierre Gilles Lemarié Rieusset. *Ondelettes à localisation exponentielle*, Journal de Mathématiques Pures et Appliquées, 67 (1988): 227-236.

[11] Tudor Barbu. *Variational image denoising approach with diffusion porous media flow*, Abstract and Applied Analysis, 2013 (2013).